

ESR study of spin dynamics in $(\text{Er}_{0.5}\text{Y}_{0.5})_2\text{Cu}_2\text{O}_5$ solid solutions

J. TYPEK^{1*}, N. GUSKOS^{1,2}

¹Institute of Physics, Szczecin University of Technology, al. Piastów 17, 70-310 Szczecin, Poland

²Solid State Physics Section, Department of Physics, University of Athens,
Panepistimiopolis, 15 784 Zografos, Athens, Greece

Powder samples of $(\text{Er}_{0.5}\text{Y}_{0.5})_2\text{Cu}_2\text{O}_5$ have been synthesized by a solid state reaction method. Electron spin resonance (ESR) measurements have been carried out on a Bruker E 500 X-band spectrometer in the 4–300 K temperature range. A single, almost Lorentzian-shaped resonance line has been recorded for the whole investigated temperature range and its ESR parameters (integrated intensity, linewidth and resonance field) displayed a strong temperature dependence. The integrated intensity of the resonance line showed a pronounced maximum in low-temperature range and vanished at the transition to the antiferromagnetic ordering at $T_N = 11$ K. The temperature at which the ESR integrated intensity reaches its maximum is different for the heating and cooling runs. Below 40 K, on approach to T_N , the linewidth exhibited a divergent behaviour due to the onset of three-dimensional magnetic order. At higher temperatures (about 220 K), variations in ESR magnetic susceptibility suggest the presence of dynamical processes in copper–oxygen chains leading to the formation of copper dimers. The observed changes of the ESR parameters are interpreted in terms of 2D magnetism of the copper–oxygen system in the $(\text{Er}_{0.5}\text{Y}_{0.5})_2\text{Cu}_2\text{O}_5$ solid solution.

Key words: ESR; spin chains; copper complex

1. Introduction

$(\text{Er}_{0.5}\text{Y}_{0.5})_2\text{Cu}_2\text{O}_5$ belongs to the family of $\text{R}_2\text{Cu}_2\text{O}_5$ compounds (R = rare earth ion smaller than Gd ion, i.e., Tb, Dy, Ho, Yb, Er, Tm, Yb, Lu, as well as Y, Sc, In) with the orthorhombic $Pna2_1$ space group symmetry [1–3]. The most characteristic feature of $\text{R}_2\text{Cu}_2\text{O}_5$ crystallographic structure is the presence of zigzag copper chains along the a -axis. A distorted square planar arrangement of four oxygen atoms around copper atom exists, with a fifth oxygen making a sort of pyramid. These copper–oxygen pyramids are joined at the common edges forming Cu_2O_8 dimers. The dimers, through

* Corresponding author; e-mail: typjan@ps.pl

the bridging oxygen, form an infinite zigzag Cu_2O_5 copper–oxygen chains. Furthermore, each copper ion is coupled to four other Cu ions along the b -axis forming ab -pseudoplanes. The rare earth ions are octahedrally coordinated and resulting distorted RO_6 octahedra are linked in a three-dimensional network occupying the space between copper–oxygen planes [3].

All $\text{R}_2\text{Cu}_2\text{O}_5$ compounds order antiferromagnetically at low temperatures, ranging from 11 K (Dy) to 30 K (In), and most of them exhibit metamagnetic behaviour below the Neel temperature [4]. The magnetic properties of $\text{Y}_2\text{Cu}_2\text{O}_5$ have been studied extensively [4–10]. Above 120 K, the magnetic susceptibility of this compound is well described by the Curie–Weiss law with a positive Curie temperature of $\theta = 38.5$ K, indicating a considerable contribution of ferromagnetic interaction [4]. At $T_N = 11.5$ K, a sharp maximum in the susceptibility gives a strong indication of an antiferromagnetic ordering. In the antiferromagnetic state two jumps in the $M(H)$ magnetization curve (with the external field H applied along b -axis) are observed, corresponding to two metamagnetic transitions [10]. The magnetic properties of $\text{Er}_2\text{Cu}_2\text{O}_5$ have been investigated previously [4, 5, 11–15]. The susceptibility follows the Curie–Weiss law exactly down to the transition temperature of $T_N = 27$ K, with a negative value of the Curie–Weiss temperature of $\theta = -4$ K (antiferromagnetic interaction) [4]. The magnetic structure in an ordered state of $\text{R}_2\text{Cu}_2\text{O}_5$ could be viewed as consisting of ferromagnetic CuO layers parallel to the ab -plane coupled antiferromagnetically with the copper magnetic moments aligned along the b -axis. These copper pseudolayers are bracketed by two Er layers having their magnetic moment antiparallel to copper magnetic moments. This indicates that the superexchange $\text{Er}^{3+}\text{–Cu}^{2+}$ is antiferromagnetic [13]. Despite a large experimental material gathered from magnetic susceptibility and neutron diffraction measurements, the nature of magnetic interactions in the $\text{R}_2\text{Cu}_2\text{O}_5$ family is still incomplete.

$(\text{R}_x\text{R}'_{1-x})_2\text{Cu}_2\text{O}_5$ solid solutions could be prepared by the solid state reaction technique. XRD, thermogravimetry and ESR at room temperatures have been used to study $(\text{Er}_x\text{Y}_{1-x})_2\text{Cu}_2\text{O}_5$, $(\text{Dy}_x\text{Y}_{1-x})_2\text{Cu}_2\text{O}_5$, and $(\text{TbxY}_{1-x})_2\text{Cu}_2\text{O}_5$ solid solutions [15–17]. Only the signal from copper(II) ions has been recorded by conventional X-band ESR spectroscopy. It was found that the relative ESR signal intensity varies with the magnetic rare earth ion concentration index x according to a simple power law function.

The aim of this work was to extend previously reported room-temperature ESR study of $(\text{Er}_{0.5}\text{Y}_{0.5})_2\text{Cu}_2\text{O}_5$ to the whole temperature range available (4–300 K) in order to gain insight into the dynamics of copper spin system. Special attention was paid to the behaviour of copper spin chains present in the $(\text{Er}_{0.5}\text{Y}_{0.5})_2\text{Cu}_2\text{O}_5$ structure in a low-temperature range, close to the transition to the antiferromagnetic phase.

2. Experimental

Ceramic sample of $(\text{ErY})_2\text{Cu}_2\text{O}_5$ has been prepared by heating an appropriate stoichiometric amounts of metal oxides in air and was described elsewhere [15].

X-ray characterization showed that the sample is single phase with the following orthorhombic lattice parameters: $a = 1.0878$ nm, $b = 0.3477$ nm, $c = 1.2446$ nm. No significant traces of copper tetramers in this sample have been observed by ESR spectroscopy.

ESR variable temperature experiments were performed with a Bruker E 500 spectrometer operating at X-band microwave frequency equipped with TE102 cavity with 100 kHz field modulation. The investigated sample was in a form of loose powder and during the measurements it was placed in a quartz tube. The sample was cooled by flowing He gas and the temperature was controlled within about 1% by using a digital temperature controller. In this paper, the resonance magnetic field B_{res} is defined as the field where the applied magnetic field derivative of the resonance absorption line becomes zero. The effective g -value, g_{eff} , was also be used, defined by the relation $h\nu = g_{\text{eff}}\mu_B B_{\text{res}}$, where μ_B is the Bohr magneton, and ν the microwave frequency. Decomposition of the observed ESR spectrum on constituent components has been done using the SIMPOW computer program.

3. Results and discussion

ESR spectra of $(ErY)_2Cu_2O_5$ at selected temperatures in high and low-temperature ranges are presented in Figs. 1 and 2, respectively. At a specific temperature, the spectrum consists of a single, almost symmetrical, Lorentzian-shape line, whose ESR amplitude increases as the temperature is decreased. Also the linewidth broadens with temperature decrease, especially very quickly in the low-temperature range. At the lowest investigated temperatures, the ESR line is very broad, intense and asymmetrical. It was also noticed that the behaviour of the spectra depends on the thermal history of the sample, in particular whether the spectrum was recorded during cooling or heating runs. The spectra, although very broad and asymmetrical, were observed down to the temperature of the appearance of an antiferromagnetic state for this sample, i.e. 11 K. Comparing this value with the published results for $Y_2Cu_2O_5$ ($T_N = 11.5$ K) and for $Er_2Cu_2O_5$ ($T_N = 27$ K) it could be deduced that the ESR signal originated only from the copper ions located in the vicinity of non-magnetic Y^{3+} ions, and not from copper ions close to the magnetic Er^{3+} ions. This is consistent with the conclusion made previously that the presence of a magnetic ion effectively switches out the copper ions in its vicinity from taking part in formation of the ESR signal [15–17]. A closer inspection of the obtained ESR spectra suggests discussion of the temperature dependence of the ESR parameters separately in the low- ($T < 50$ K), intermediate- ($50 < T < 175$ K) and high- ($T > 175$ K) temperature ranges.

In the low-temperature range, critical behaviour of the ESR parameters (linewidth, g -factor, integrated intensity) due to approaching to the antiferromagnetic phase tran-

sition, is expected. Figure 3 presents the temperature dependence of the effective peak-to-peak linewidth, ΔB_{eff} below 50 K.

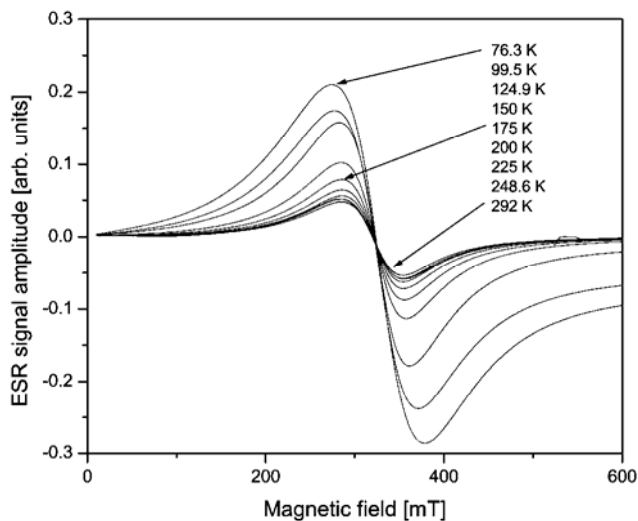


Fig. 1. ESR spectra of $(\text{ErY})_2\text{Cu}_2\text{O}_5$ at selected temperatures in the high-temperature range ($T > 60$ K)

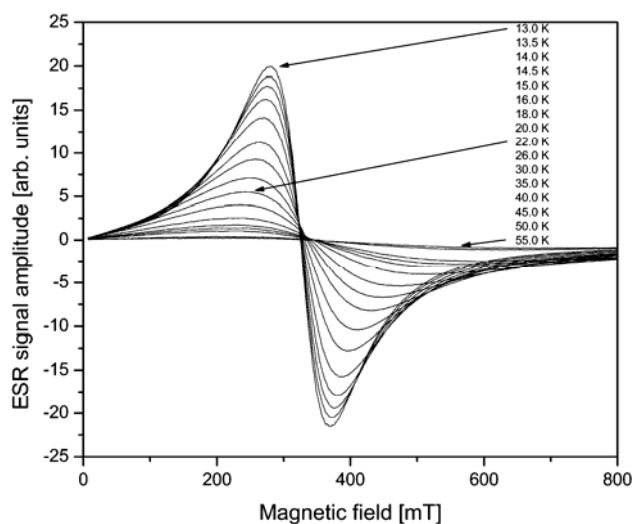


Fig. 2. ESR spectra of $(\text{ErY})_2\text{Cu}_2\text{O}_5$ at selected temperatures in the low-temperature range ($T < 60$ K)

A sharp increase in the linewidth with decreasing temperature is indicative of cooperative character of the magnetic ordering and can be explained by magnetic fluctuations in the vicinity of the transition temperature. It is reasonable to analyse this dependence in terms of the reduced temperature $(T - T_N)/T_N$, where T_N is the Neel

temperature at which the sample undergoes a long-range antiferromagnetic ordering. As the linewidth is expected to follow a power law dependence on reduced temperature, the experimental results have been fitted (Fig. 3) with the function

$$\Delta B_{\text{eff}} = \Delta B_0 + A \left(\frac{T - T_N}{T_N} \right)^{-p} \quad (1)$$

where ΔB_0 and A are temperature independent constants, and p is the critical exponent for the linewidth.

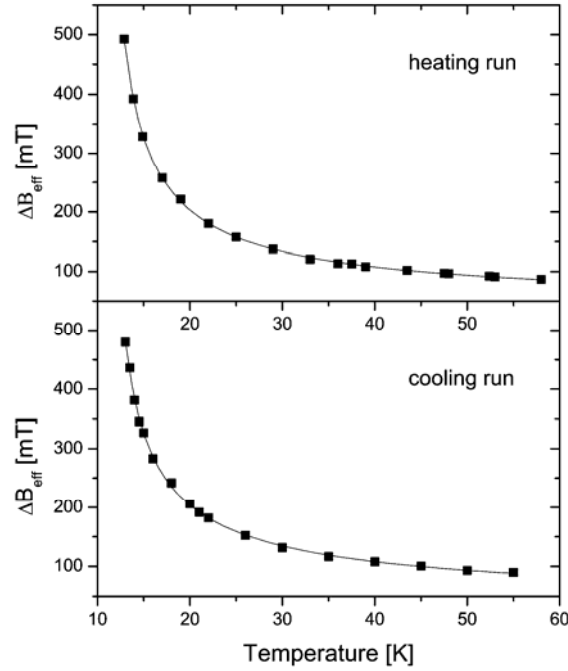


Fig. 3. Temperature dependences of the effective linewidth, ΔB_{eff} , in the low-temperature range for the cooling and heating runs. Experimental points (full squares) have been fitted with Eq. (1) (solid line)

Equation (1) describes a critical line broadening during the antiferromagnetic ordering in many 3D and non-ideal low-dimensional magnetic compounds. As the ESR spectrum of $(Er_{0.5}Y_{0.5})_2Cu_2O_5$ at a specific temperature suggested dependence on whether the measurement was done during the cooling or heating run, the fitting was done separately for these runs. The least-squares fitting gave the following values in Eq. 1: $\Delta B_0 = 26(15)$ mT, $A = 162(10)$ mT, $T_N = 10.7(4)$ K, and $p = 0.68(9)$ for the cooling run; $\Delta B_0 = 39(5)$ mT, $A = 158(2)$ mT, $T_N = 10.2(2)$ K, and $p = 0.78(4)$ for the heating run. Although different values were obtained for the Neel temperature and the critical exponent, the difference might be apparent resulting from the uncertainties

only. The calculated value of $p \approx 0.74$ reflects the low-dimensional character of the ESR line when it is compared with the critical behaviour of ΔB in typical 1D anti-ferromagnets, such as $\text{CuCl}_2 \cdot 2 \text{NC}_5\text{H}_5$ ($p = 0.5$), $\text{Sr}_2\text{V}_3\text{O}_9$ ($p = 1$), or in the 3D case, such as GdB_6 ($p = 1.5$) [18]. Furthermore, it was shown that in the low-dimensional spin systems an essential broadening can occur in a rather broad temperature range of about $1.5T_N < T < 10T_N$.

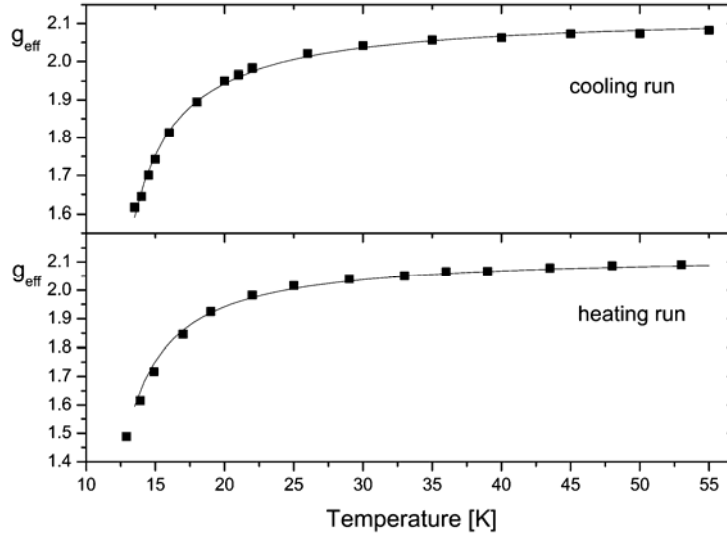


Fig. 4. Temperature dependences of the effective g -factor, g_{eff} , in the low-temperature range, for the cooling and heating runs. Experimental points (full squares) have been fitted with the function (2) (solid line)

Figure 4 presents temperature dependences of the effective g -factor, g_{eff} , below 50 K for cooling and heating runs. Because the resonance line shifts to a higher magnetic field with decreasing temperature, the the g -factor shifts to lower values, implying a rapid evolution of a short-range antiferromagnetic order. This negative deviation in g -value is predicted for a system dominated by spin symmetric exchange, when the magnetic field is applied parallel to the chain direction [19]. Many studies of the copper spin systems devoted to the thermal behaviour of the g -factor have found the shift that was proportional to reciprocal temperature, e.g. in single crystals of the copper salt of l-alanine amino acid $\text{Cu}[\text{NH}_2\text{CH}(\text{CH}_3)\text{CO}_2]_2$ [20]. The observed shift was explained by the polarization of the spin system induced by the external magnetic field when the temperature is lowered. Thus the thermal behaviour of g_{eff} in $(\text{Er}_{0.5}\text{Y}_{0.5})_2\text{Cu}_2\text{O}_5$ has been simulated with the following function

$$g(T) = g_0 - c \left(\frac{T - T_N}{T_N} \right)^{-q} \quad (2)$$

where g_0 and c are temperature-independent parameters, T_N is the Neel temperature, and q the critical exponent for the g -factor. The least-squares fitting produced satisfactory results and the following values of the parameters in Eq. (2) were obtained; for the heating run: $g_0 = 2.12(2)$, $c = 0.20(5)$, $T_N = 9.5(1.4)$ K, $q = 1.1(3)$; for the cooling run: $g_0 = 2.13(1)$, $c = 0.18(1)$, $T_N = 10.2(1.4)$ K, $q = 1.01(6)$. Also in this case both sets of parameters seem to be the same within experimental errors. The most important result of this fitting is that the value of the critical exponent for the g -factor is equal to unity, i.e., the factor is inversely proportional to temperature.

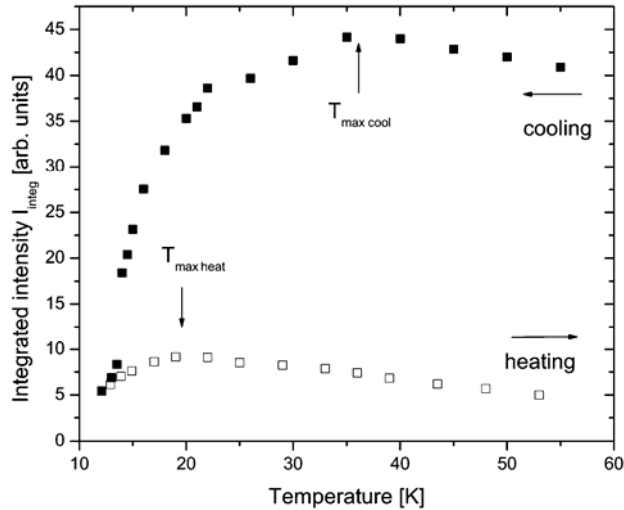


Fig. 5. Temperature dependences of the integrated intensity, I_{integ} , during the cooling (full squares) and heating (empty squares) runs in the low-temperature range

Another important ESR parameter is the integrated intensity, I_{integ} , defined as the area under the ESR absorption curve. In the paramagnetic regime, I_{integ} is proportional to the static susceptibility of spins participating in the resonance. Figure 5 presents the temperature dependences of I_{integ} in the low-temperature range for the cooling and heating runs. Clear maxima of I_{integ} is to be observed for both runs but at significantly different temperatures. During the cooling run, the maximum is reached at 36 K, while during the heating run much smaller values of I_{integ} are observed and the maximum is seen at 19 K. The appearance of maxima of the integrated intensity (and thus spin susceptibility) at temperatures different from T_N is a clear manifestation of a low-dimensional magnetic system. An empirical criterion for determination of the magnetic dimensionality is offered by the ratio T_N/T_{max} , where T_{max} is the temperature of the maximum susceptibility [21]. For 1D magnetic systems, $T_N/T_{\text{max}} < 0.1$, for 2D systems $0.25 < T_N/T_{\text{max}} < 0.5$, and $T_N/T_{\text{max}} > 0.9$ for 3D magnets. Applying this criterion to our spin system, it could be concluded that $(Er_{0.5}Y_{0.5})_2Cu_2O_5$ is a 2D magnetic system.

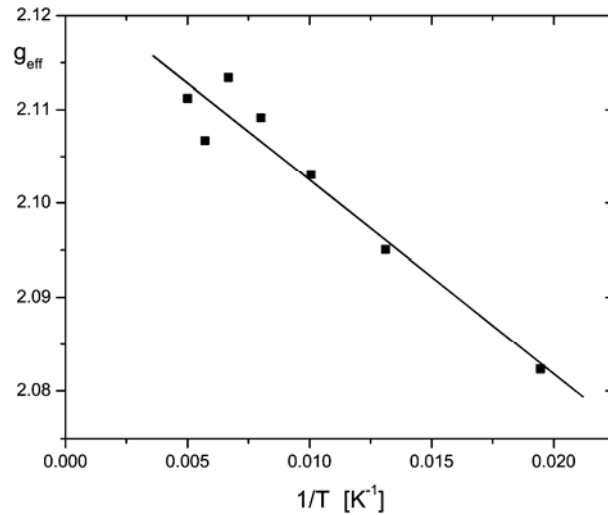


Fig. 6. Temperature dependence of the effective g -factor, g_{eff} , in the intermediate temperature range. The data are plotted as a function of inverse temperature to show the linear behaviour

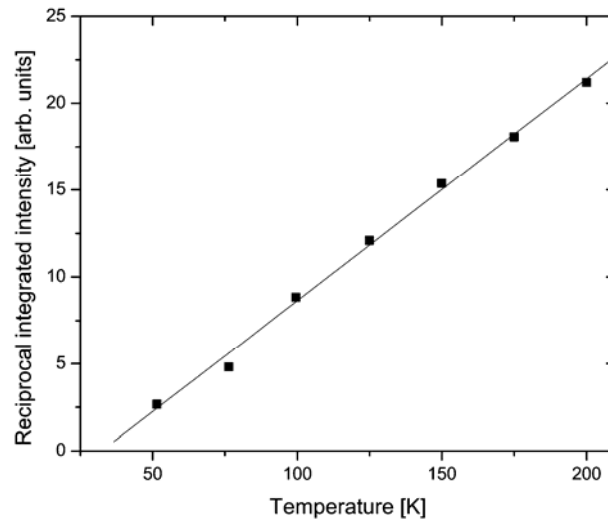


Fig. 7. Temperature dependence of the reciprocal integrated intensity in the intermediate temperature range

In the intermediate temperature range the ($50 \text{ K} < T < 200 \text{ K}$), the effective linewidth and g -factor follow the same temperature dependences as in the low-temperature range, i.e. Eqs. (1) and (2), respectively. Figure 6 demonstrates this for the temperature behaviour of the g -factor. There is a clear linear dependence between T^{-1} and g_{eff} also in this temperature range. The integrated intensity follows the Curie–Weiss law, $I_{\text{integ}} = C/(T - \Theta)$, where C and Θ are the Curie constant and Curie–Weiss

temperature, respectively. Least-squares fitting of the experimental data gave $\Theta = 32(2)$ K (Fig. 7). The positive sign of the Curie–Weiss temperature is an evidence for ferromagnetic interactions between copper paramagnetic centres.

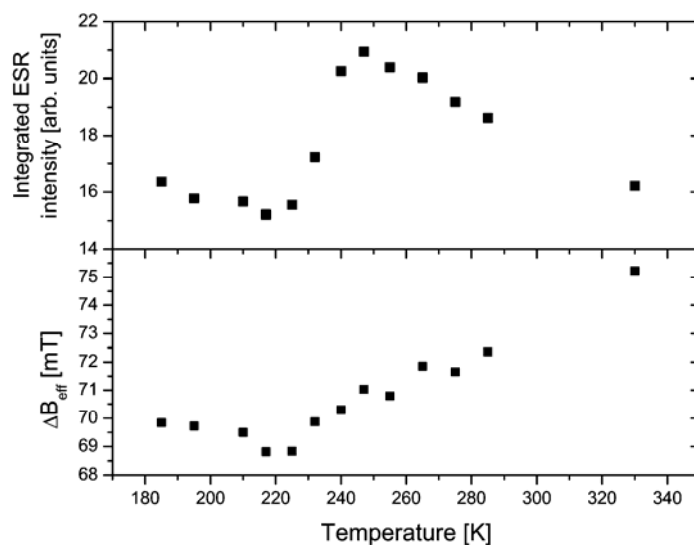


Fig. 8. Temperature dependence of the integrated intensity (upper panel) and effective linewidth (lower panel) in the high-temperature range

In the high-temperature range, an unexpected behaviour of the integrated intensity and linewidth is observed (Fig. 8). On the background of steady decrease of the integrated intensity extending from the intermediate temperature range, a rather abrupt increase above 220 K is seen (Fig. 8, upper panel). At the same temperature, the linewidth reverses its trend of decreasing with the temperature and begins to increase (Fig. 8, lower panel). I_{integ} reaches a local maximum at 245 K and continues to decline upon a further temperature increase. This local peak in thermal dependence of the integrated intensity could be connected with the presence of a small number of isolated copper dimers forming $-\text{Cu}-\text{Cu}-\text{O}-\text{Cu}-\text{Cu}-\text{O}-$ spin chains. At high enough temperatures, $T > 400$ K, the spins are expected to behave as $S = 1/2$. When the short-range order develops in this compound as a result of decreasing T , a pair of two spins which antiferromagnetically couple is expected to behave as a spin with $S = 0$. The number of the pairs (each pair could be regarded as a singlet dimer) increases with decreasing T , what is producing decreases of the integrated intensity, as most dimers fall into nonmagnetic $S = 0$ ground state.

Below 220 K the dimers are not recorded by the ESR spectrometer. The increase of observed linewidth above the same temperature may be the result of existence of an additional relaxation channel (through dimer subsystem) in high temperatures.

ESR of powder samples provides only limited information about the investigated specimens due the availability of only averaged magnetic characteristics. Computer

simulation programs might help to resolve the observed powder spectrum into its anisotropic g -factors and ΔB_i components. We have used the SIMPOW program and were able to make the decomposition of spectra recorded at temperatures higher than 25 K. For lower temperatures, the spectra of $(\text{Er}_{0.5}\text{Y}_{0.5})_2\text{Cu}_2\text{O}_5$ were too anisotropic, probably due to the admixture of non-diagonal terms in dynamic susceptibility [22]. The result of decomposition is presented in Fig. 9. The upper panel presents temperature dependences of three ΔB_i linewidths, while the middle and lower panels – three g_i -factors. The middle panel displays the same g_i -factors, but on reduced scales to present small variations, not visible in the lower panel. As could be easily noticed, already at temperature as high as 175 K, the g_i -factors start to differ, although drastic differences are observed only below 30 K. Thus one can conclude that the local internal field, produced by local order of copper spins, develops at temperatures much higher than T_N . It is interesting to note the behaviour of g -factors close to T_N : the shift of g_x -factor, from the high-temperature value of 2.1 to low-temperature 1.6, is roughly twice as large as the shift of g_z to higher values (from 2.1 to 2.4).

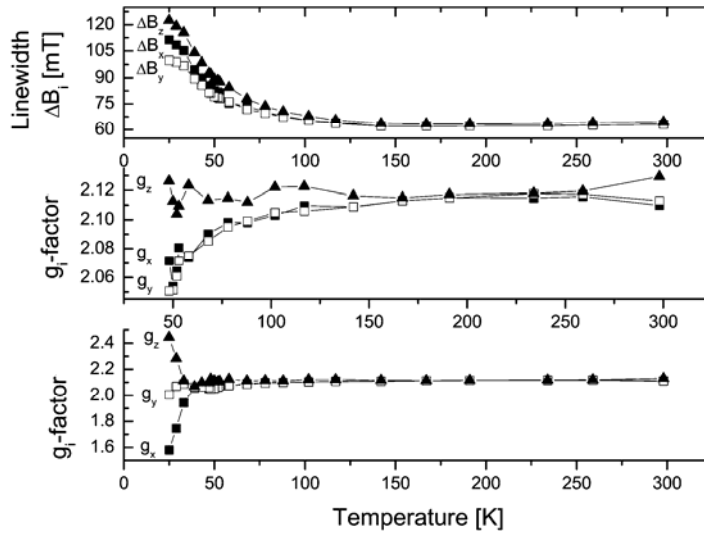


Fig. 9. Temperature dependences of three linewidths ΔB_i (upper panel) and g_i -factors (middle and lower panels) of the decomposed ESR spectrum. The middle panel presents only part of the lower panel graph, but in reduced g -factor scales

The theory of thermal shifts of g -factors in low-dimensional magnetic systems has been presented in Ref. 21. For an infinite 1D spin chain the fractional shift $\partial g(T)$ is

$$\partial g(T) = -\frac{C_1}{T} (1 - 3 \cos^2 \theta) \quad (3)$$

where θ is the angle between the applied field and the chain axis, C_1 is a constant depending on lattice parameters. The maximum shift is for $\theta = 0^\circ$. It is reduced to a half

and changes its sign for $\theta = 90^\circ$, while it vanishes for ‘the magic angle’ $\theta = 54.75^\circ$. For a 2D square planar lattice one obtains

$$\partial g(T) = \frac{C_2}{T} (1 - 3 \cos^2 \theta) \quad (4)$$

where θ is the angle between the applied field B and the normal to the spin layer. A positive shift is expected whenever B is within the layer ($\theta = 90^\circ$), doubling this value and changing sign for B along the normal to the layer. For 3D simple cubic lattice, no shifts are expected. Comparison of the shifts of the experimental g -factor in $(Er_{0.5}Y_{0.5})_2Cu_2O_5$ with theoretical predictions clearly indicates on the 2D magnetic case. Thus g_x plays a role of g -factor perpendicular the Cu ab -pseudoplanes, that is along c -axis.

4. Conclusions

ESR signals follow the magnetic activity of only the copper subsystems in $(Er_{0.5}Y_{0.5})_2Cu_2O_5$ solid solution. The transition to the antiferromagnetic state at $T_N = 11$ K is accompanied by a critical behaviour of the ESR parameters. Local ordering of magnetic spins starts already at 175 K. Part of copper ions are involved in dimer formation with the $S = 0$ ground state unobserved by the ESR method. In general, there is a strong spectroscopic evidence for the 2D magnetism in the investigated compound. Extension of the this type of study to other $(R'_xY_{1-x})_2Cu_2O_5$ solid solutions might clarify the remaining problems.

References

- [1] BERGERHOFF G., KASPER H., Acta Crystallogr., B 24 (1968), 388.
- [2] FREUD H.R., MULLER-BUSCHBAUM H., Z. Naturforsch., B 32 (1977), 609.
- [3] GARCIA-MUNOZ J.L., RODRIGUEZ-CARVAJAL J., J. Solid State Chem., 86 (1990), 310.
- [4] TROĆ R., KLAMUT J., BUKOWSKI Z., HORYŃ R., STĘPIEŃ-DAMM J., Physica B, 154 (1989), 189.
- [5] KAZEI Z.A., KOLMAKOVA N.P., LEVITAN R.Z., MILL B.V., MOSHCHALOV V.V., ORLOV V.N., SNEGIREV V.V., ZOUBKOVA JA., J. Magn. Magn. Mater., 86 (1990), 124.
- [6] GARCIA-MUNOZ J.L., RODRIGUEZ-CARVAJAL J., OBRADORS X., VALLET-REGI M., GONZALEZ CALBET J., GARCIA E., Phys. Lett., A 149 (1990), 319.
- [7] HORYŃ R., KLAMUT J., WOŁCYRZ M., WOJAKOWSKI A., ZALESKI A.J., Physica B, 205 (1995), 51.
- [8] BARAN M., LEVITIN R.Z., MILL B.V., SZYMCZAK R., Zh. Eksp. Teor. Fiz., 109 (1996), 961.
- [9] SZYMCZAK R., SZYMCZAK H., BARAN M., LEVITIN R.Z., MILL B.V., J. Magn. Magn. Mater., 157–158 (1996), 667.
- [10] MATSUOKA Y., NISHIMURA Y., MITSUDO S., NOJIRI H., KOMATSU H., MOTOKAWA M., KAKURAI K., NAKAJIMA K., KARASAWA Y., NIIMURA N., J. Magn. Magn. Mater., 177–181 (1998), 729.
- [11] ZOUBKOVA YA., KAZEI Z.A., LEVITIN R.Z., MILL B.V., MOSHCHALOV V.V., SNEGIREV V.V., Pisma Zh. Exp. Teor. Fiz., 49 (1989), 524.

- [12] PLAKHTII V.P., BONNE M., GOLOSOVSKI I.V., MILL B.V., RUDO E., FEDOROVA E.I., Pisma Zh. Exp. Teor. Fiz., 51 (1990), 637.
- [13] GARCIA-MUÑOZ J.L., RODRIGUEZ-CARVAJAL J., OBRADORS X., VALLET-REGI M., GONZALEZ-CALBET J., PARRAS M., Phys. Rev. B, 44 (1991), 4716.
- [14] SZYMCZAK R., SZYMCZAK H., BARAN M., LEVITIN R.Z., MILL B.V., J. Magn. Magn. Mater., 157–158 (1996), 667.
- [15] TYPEK J., KOSTRZEWA J., SZYMCZYK A., GUSKOS N., Mol. Phys. Rep., 39 (2004) 233.
- [16] TYPEK J., BUCHOWSKI D., GUSKOS N., SZYMCZYK A., WABIA M., Rad. Eff. Def. Solids, 158 (2003) 105.
- [17] TYPEK J., KOSTRZEWA J., GUSKOS N., Mater. Sci.-Poland, 23 (2005), 929.
- [18] IVANISHIN V.A., YUSHANKHAI V., SICHELSCHEMIDT J., ZAKHAROV D.V., KAUL E.E., GEIBEL C., Phys. Rev. B, 68 (2003), 064404.
- [19] NAGATA K., TAZUKE Y., J. Phys. Soc. Jpn., 32 (1972), 337.
- [20] CALVO R., PASSEGGI M.C.G., Phys. Rev. B, 44 (1991), 5111.
- [21] JACOBS I.S., BRAY J.W., HART H.R., INTERRANTE L.V., KASPAR J.S., WATKINS G.D., PROBER D.E., BONNER J.C., Phys. Rev. B, 14 (1976), 3036.
- [22] BENNER H., BRODEHL M., SEITZ H., WIESE J., J. Phys. C: Solid State Phys., 16 (1983), 6011.

Received 9 September 2005

Revised 23 November 2005